

Scanning probe nanolithography - Direct fabrication of mesoscopic devices

U. F. Keyser¹, H. W. Schumacher¹, U. Zeitler¹, R. J. Haug¹, K. Eberl²

¹ Institut für Festkörperphysik, Universität Hannover, Appelstr. 2, D-30167 Hannover, Germany
e-mail: keyser@nano.uni-hannover.de

² Max-Planck-Institut für Festkörperforschung, Heisenbergstr. 1, D-70569 Stuttgart, Germany

Abstract We are using an atomic force microscope for the direct fabrication of low-dimensional quantum structures in GaAs/AlGaAs-heterostructures. With the combination of nanomachining and current-controlled local oxidation we can design devices such as a single-electron transistor. Our step-by-step fabrication process enables us to test the devices at low temperatures after every step of the nanolithography. Here we present experiments on systems with 2D-0D-2D and 2D-1D-2D tunneling characteristics. We observe a charging effect in the characteristics of a tuneable resonant tunneling device which is explained by asymmetric tunneling barriers.

1 Introduction

The atomic force microscope (AFM) is a promising tool for the fabrication of small semiconductor devices. The small probe of the AFM allows to influence the sample properties on a length scale of below 10 nm by applying either a high force to the tip to mechanically remove atoms or a high voltage to oxidate the surface. Several groups used a scanning probe microscope to produce etch masks on silicon [1], to pattern photoresist [2] or to directly change the band structure in GaAs-AlGaAs-heterostructures with one of the above techniques [3–6].

2 Fabrication

We are using a commercial AFM with conductive silicon tips. The 2DEG is situated 40 nm below the surface of a modulation doped AlGaAs/GaAs heterojunction (grown by molecular beam epitaxy) consisting of 500 nm GaAs, 15 nm undoped AlGaAs, 15 nm of Si doped AlGaAs, 5 nm undoped AlGaAs and a 5 nm thick GaAs cap layer (sheet density $n = 4 \times 10^{15} \text{ m}^{-2}$, mobility $\mu = 23 \text{ m}^2/\text{Vs}$).

After the fabrication of a Hall bar geometry with Au/Ge/Ni Ohmic contacts the samples are contacted and mounted into the AFM. First the controlled nanomachining [5] is done to define in plane gates (IPG). Then follows a test of the such fabricated field effect transistor at liquid helium temperature. If inhomogenities are incorporated in the IPG-channel the device is excluded from further processing. After this characterization step the sample is again mounted into the AFM and a single-electron transistor (SET) is defined by adding two tunneling barriers formed by local oxidation. We are using current-controlled local oxidation to tune the height of the tunneling barriers connecting the SET-island to the source-drain contacts. The barrier heights Φ^{eff} can be reproducibly adjusted between a few meV and more

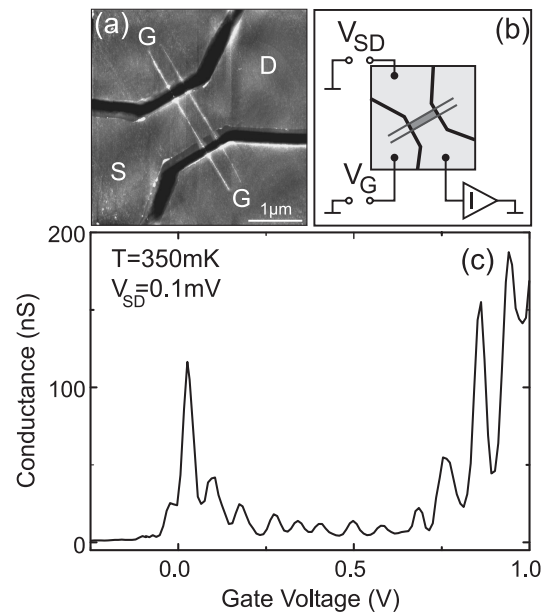


Fig. 1 (a) AFM-micrograph of Sample 1 (SET) with source-drain contacts (S,D) and in plane gates (G) - (b) measurement setup - (c) Coulomb-blockade oscillations of the quantum dot in (a) at $T = 350 \text{ mK}$.

than a hundred meV by applying different oxidation currents [7]. Fig. 1(a) shows a such fabricated quantum dot (electronic dimensions: 500 nm x 250 nm) in the following addressed as Sample 1. Both tunneling barriers were written with a constant oxidation current $I_{OX} = 150 \text{ nA}$ (writing speed 250 nm/s). This corresponds to an electronic height for the barriers $\Phi^{eff} \approx 15 \text{ meV}$ [7], the lines are separated by 250 nm .

3 Measurements

At $T = 350 \text{ mK}$ the typical Coulomb-blockade oscillations (Fig. 1(c)) are observed for Sample 1 by applying a constant source-drain voltage and sweeping one of the IPGs (Fig. 1(b)). By analyzing the Coulomb-blockade diamonds (for details see [7]) we can estimate the diameter of the dot to be $\approx 300 \text{ nm}$ which is comparable to the dimensions estimated from the AFM image when taking into account the depletion length of the IPGs ($\approx 300 \text{ nm}$).

To investigate the transition from 2D-0D-2D to a 2D-1D-2D resonant tunneling device we fabricated a wider

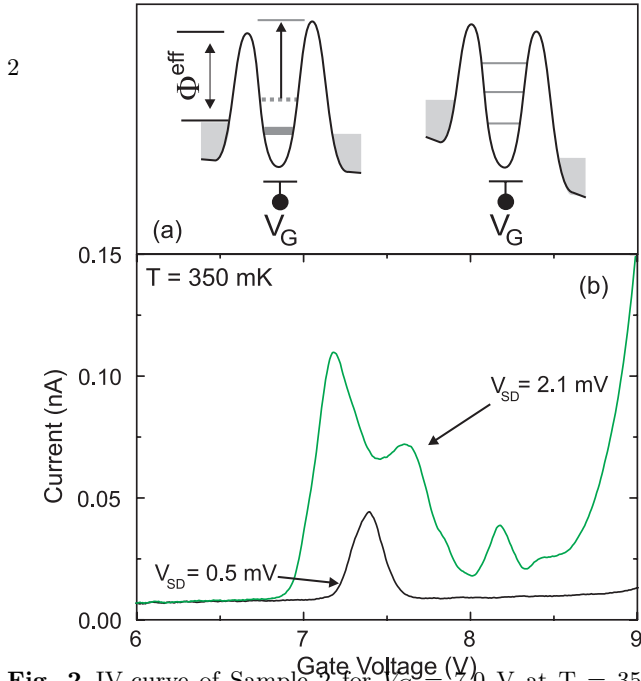


Fig. 2 IV-curve of Sample 2 for $V_G = 7.0$ V at $T = 350$ mK shows clear negative differential resistance - Inset: AFM-micrograph of Sample 2.

IPG-channel ($2.0 \mu\text{m}$) on the same heterostructure. We used similar writing parameters for the double-barrier structure as for Sample 1 ($I_{OX} = 150$ nA, tunneling barrier distance 250 nm) though another AFM-tip was used. The inset of Fig. 2 shows an AFM-micrograph of the new device (electronic dimensions: $2.0 \mu\text{m} \times 250$ nm - Sample 2). In Fig. 2 the IV-curve for a gate voltage $V_G = 7.0$ V is shown. Two clear peaks with negative differential resistance (NDR) in both bias directions are observed and indicate a 2D-1D-2D tunneling process through a one-dimensional quantum wire as observed in Schottky-gated field effect transistors [8] or vertical resonant tunneling structures [9]. The double-barrier structure is asymmetric because it is not centered in the IPG-channel (with respect to the current direction). The peak-to-peak distance in forward (reverse) bias direction is about 4 mV (3 mV) and the maximal peak-to-valley ratio is 1.4 (at $V_G = 6.0$ V not shown). Assuming a voltage to energy conversion factor of ≈ 0.5 the energy separation of the two subbands lies between 1.5 meV and 2.0 meV. By a one-dimensional numerical calculation of a double-barrier structure with gaussian tunneling barriers ($\Phi^{eff} = 15$ meV, FWHM = 140 nm) we obtain typical energy-spacings of 1.6 meV.

In contrast to Sample 1 the IPG-characteristic of Sample 2 exhibits only one peak (Fig. 3(b)) at low bias voltage ($V_{SD} = 0.4$ mV) but more peaks appear at higher bias voltages $V_{SD} > 1.0$ mV. The suppression of the peaks at low bias voltage may indicate a charging effect. This is illustrated in Fig. 3(a) by two sketches of the conduction band for two different bias voltages of Sample 2. The tunneling current is determined by the tunneling rate through the higher barrier. At low bias the electrons first pass the left (low) then the right (high) tunneling barrier and thus are injected faster than they can leave the quantum wire. The accumulation of the electrons at the right barrier shifts the energy of all but the lowest

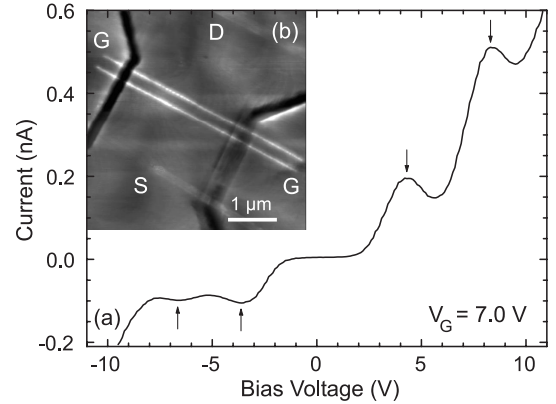


Fig. 3 (a) By applying a higher V_{SD} the asymmetry of the tunneling barriers is inverted (b) IPG-characteristics at $T = 350$ mK, at $V_{SD} = 0.4$ mV only one peak is observed at $V_{SD} > 1.0$ mV more peaks appear.

1D-subbands to higher energies. By applying higher bias voltages more states can take part in the transport and more peaks are observed in the source-drain current.

4 Conclusions

The AFM nanolithography is a promising technique for the fabrication of low-dimensional devices, this technique provides control over all the steps needed in the processing of a sample. The device tunneling characteristics (2D-1D-2D, 2D-0D-2D) are determined by the width of the in-plane gate channel. It is possible to fabricate single electron transistors and tuneable resonant tunneling diodes with well defined properties.

References

1. E. S. Snow, W. H. Juan, S. W. Pang, and P. M. Campbell, Appl. Phys. Lett. **66**, (1995) 1729.
2. B. Klehn, S. Skaberna, and U. Kunze, Superl. and Microstructures **25**, (1998) 473.
3. M. Ishii, and K. Matsumoto, Jpn. J. Appl. Phys. Lett. **34**, (1995) 1329.
4. R. Held, T. Vancura, T. Heinzl, K. Ensslin, M. Holland, and W. Wegscheider, Appl. Phys. Lett. **73**, (1998) 262.
5. H. W. Schumacher, U. F. Keyser, U. Zeitler, R. J. Haug, and K. Eberl, Appl. Phys. Lett. **75**, (1999) 1107.
6. Y. Okada, Y. Iuchi, M. Kawabe, and J. S. Harris Jr., J. Appl. Phys., Part 2 **38**, (1999) 160.
7. U. F. Keyser, H. W. Schumacher, U. Zeitler, R. J. Haug, and K. Eberl, Appl. Phys. Lett. **76**, (2000) 457.
8. K. Ismail, D. A. Antoniadis, and H. I. Smith, Appl. Phys. Lett. **55**, (1989) 589.
9. J. Wang, P. H. Beton, N. Mori, H. Buhmann, L. Mansouri, L. Eaves, P. C. Main, T. J. Foster, and M. Henini, Appl. Phys. Lett. **65**, (1994) 1124.